Journal of Medicinal Chemistry

Article

pubs.acs.org/jmc

3-Aryl-[1,2,4]triazino[4,3-*a*]benzimidazol-4(10*H*)-one: A Novel Template for the Design of Highly Selective A_{2B} Adenosine Receptor Antagonists

Sabrina Taliani,*[,†] Isabella Pugliesi,[†] Elisabetta Barresi,[†] Francesca Simorini,[†] Silvia Salerno,[†] Concettina La Motta,[†] Anna Maria Marini,[†] Barbara Cosimelli,[‡] Sandro Cosconati,[§] Salvatore Di Maro,[‡] Luciana Marinelli,[‡] Simona Daniele,[∥] Maria Letizia Trincavelli,[⊥] Giovanni Greco,[‡] Ettore Novellino,[‡] Claudia Martini,[⊥] and Federico Da Settimo[†]

[†]Dipartimento di Scienze Farmaceutiche, Università di Pisa, Via Bonanno 6, 56126 Pisa, Italy

[‡]Dipartimento di Chimica Farmaceutica e Tossicologica, Università di Napoli "Federico II", Via D. Montesano, 49, 80131 Napoli, Italy

[§]Dipartimento di Scienze Ambientali, Seconda Università di Napoli, Via Vivaldi 43, 81100 Caserta, Italy

[∥]Department of Drug Discovery and Development, Istituto Italiano di Tecnologia, Via Morego 30, 16163 Genova, Italy

[⊥]Dipartimento di Psichiatria, Neurobiologia, Farmacologia e Biotecnologie, Università di Pisa, Via Bonanno 6, 56126 Pisa, Italy

Supporting Information

ABSTRACT: In an effort to identify novel ligands possessing high affinity and selectivity for the A_{2B} AR subtype, we further investigated the class of 3-aryl[1,2,4]triazino[4,3-*a*]benzimidazol-4(10*H*)-ones **V**, previously disclosed by us as selective A_1 AR antagonists. Preliminary assays on a number of triazinobenzimidazoles derived from our "in-house" collection revealed that all the derivatives selected showed significant affinity at A_{2B} AR, no affinity at A_3 AR, and various degrees of selectivity toward A_1 and A_{2A} ARs. Investigation of a new series featuring modified substituents at the 10-position (4′-chlorophenyl or phenylethyl groups), and a chlorine atom at the 7-position (X) of the triazinobenzimidazole nucleus, yielded highly potent and selective A_{2B} AR antagonists. The presence of a pendant 3-phenyl ring appears to hamper the interaction with A_{2A} AR, conferring high A_{2B}/A_{2A} AR selectivity. Derivative **13** (X = Cl, R = C_6H_5) is the most potent and selective compound, with an IC_{50} of 3.10 nM at A_{2B} AR and no affinity at A_1, A_{2A}, and A_3 ARs.

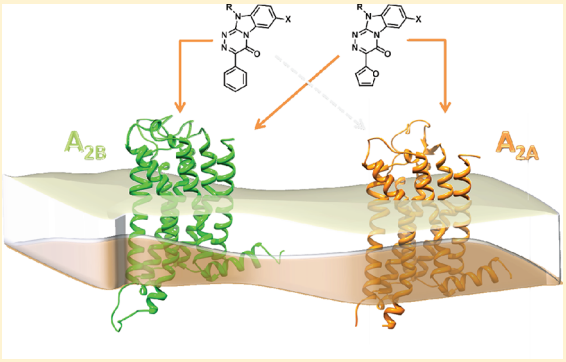

INTRODUCTION

Adenosine is an endogenous purine nucleoside that plays a key role in numerous important physiological functions through interactions with specific cell-surface G-protein-coupled receptors (GPCRs), which are classified into four subtypes, namely A_1, A_{2A}, A_{2B}, and A_3 adenosine receptors (ARs).[1−3] Responses to activation of ARs are mediated by different secondary messenger systems, such as adenylate cyclase, calcium or potassium channels (A_1 AR), phospholipase C (A_1, A_{2B}, and A_3 ARs), and phospholipase D (A_3 AR).[4]

A_{2B} ARs have been generally defined as "low-affinity ARs" due to their low affinity not only for the endogenous ligand but also for several typical agonists, such as 5′-(*N*-ethylcarboxamide)adenosine (NECA), N^6-(*R*)-phenylisopropyladenosine (R-PIA), and 2-{[4-(2-carboxyethyl)phenylethyl]-amino}-5′-*N*-ethylcarboxamidoadenosine (CGS21680), in contrast with other AR subtypes.[5,6] Under physiological conditions, extracellular adenosine reaches a concentration of approximately 100 nM and is thus able to interact only with the high-affinity A_1 and A_{2A} ARs. However, adenosine normally increases under conditions of hypoxia, ischemia, or high metabolism that typically occur in pathological or stressful situations and can grow to very high micromolar concentrations and thus activate the low affinity A_{2B} and A_3 AR subtypes.

A_{2B} AR activation implies stimulation of adenylate cyclase and activation of phospholipase C through coupling to Gs and $Gq_{/11}$ proteins, respectively, producing an increase in intracellular cAMP and calcium ion levels.[7] A_{2B} AR subtype is highly conserved among species (i.e., human (*h*) A_{2B} AR shares 86−87% amino acid sequence homology with the rat and mouse ARs)[5] and is primarily expressed in the gastrointestinal tract, bladder, lung, and on mast cells but also in the eye, adipose tissues, brain, kidney, liver, and other tissues.[3]

Numerous studies have shown that A_{2B} ARs play a crucial role in the regulation of a wide range of physiopathological

Received: August 3, 2011
Published: January 18, 2012

dx.doi.org/10.1021/jm201177b | *J. Med. Chem.* 2012, 55, 1490−1499

Chart 1. Structure of Known and Newly Synthesized A_{2B} AR Antagonists

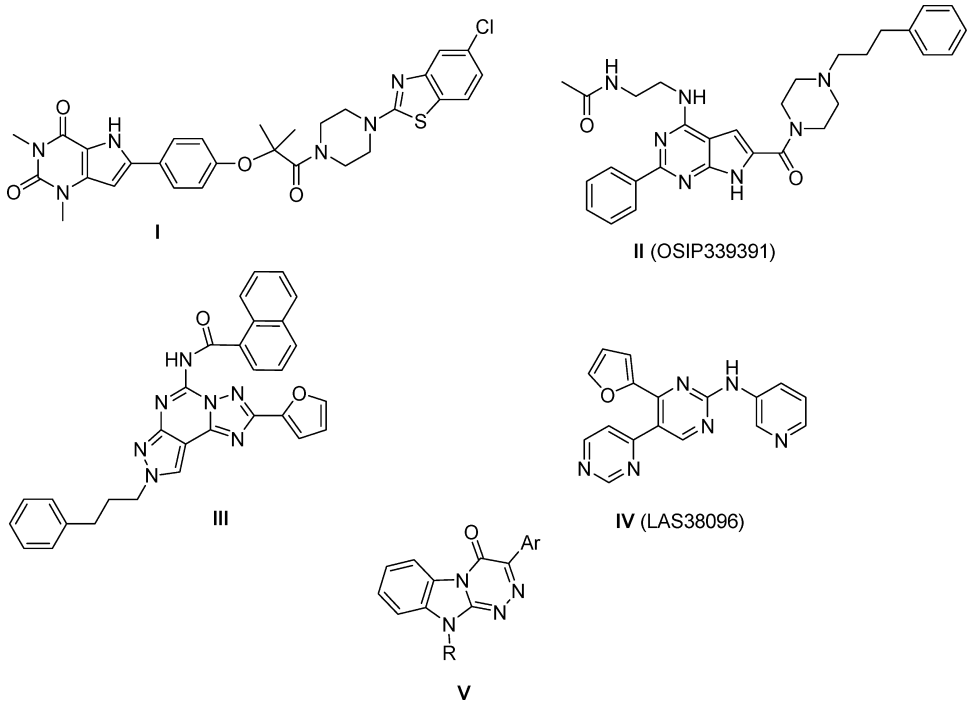

Table 1. Affinities at Human A_1, A_{2A}, A_{2B}, and A_3 ARs of Derivatives 1−14

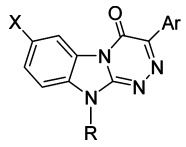

no.	X	R	Ar	hA_1 K_i (nM)[a,b]	hA_{2A} K_i (nM)[a,c]	hA_{2B} IC_{50} (nM)[a,d]	hA_3 K_i (nM)[a,e]
1[f]	H	H	C_6H_5	728 ± 38	>10000	1.40 ± 0.21	>1000
2	H	H	fur-2-yl	25.0 ± 2.4	33.0 ± 3.3	15.3 ± 1.9	>1000
3[f]	H	CH_3	C_6H_5	62.0 ± 4.0	>10000	58.0 ± 3.4	>1000
4	H	CH_3	fur-2-yl	211 ± 21	2608 ± 261	20.4 ± 3.3	>1000
5[f]	H	C_6H_5	C_6H_5	83.0 ± 6	>10000	15.0 ± 2.4	>1000
6	H	C_6H_5	fur-2-yl	>10000	3277 ± 154	3200 ± 120	>1000
7	H	C_6H_4-4-Cl	C_6H_5	1357 ± 120	>10000	2.42 ± 0.16	>1000
8	H	C_6H_4-4-Cl	fur-2-yl	>10000	50.6 ± 5.1	2.11 ± 0.04	702 ± 69
9[f]	H	$CH_2C_6H_5$	C_6H_5	299 ± 16	>10000	54.3 ± 6.9	>1000
10	H	$CH_2C_6H_5$	fur-2-yl	>10000	156 ± 14	10.0 ± 1.35	>1000
11	H	$(CH_2)_2C_6H_5$	C_6H_5	>10000	>10000	2.50 ± 0.77	328 ± 30
12	H	$(CH_2)_2C_6H_5$	fur-2-yl	>10000	15.8 ± 1.7	5.34 ± 0.81	>1000
13	Cl	C_6H_5	C_6H_5	>10000	>10000	3.10 ± 0.10	>1000
14	Cl	C_6H_5	fur-2-yl	>10000	>10000	7850 ± 1570	>1000
DPCPX				0.5 ± 0.03	337 ± 28		>1000
NECA				14 ± 4	16 ± 3		73 ± 5
CI-IBMECA				890 ± 61	401 ± 25		0.22 ± 0.02

[a]The data are expressed as means ± SEM derived from an iterative curve-fitting procedure (Prism program, GraphPad, San Diego, CA). [b]Displacement of specific [^{3}H]DPCPX binding in membranes obtained from hA_1 AR stably expressed in CHO cells. [c]Displacement of specific [^{3}H]NECA binding in membranes obtained from hA_{2A} AR stably expressed in CHO cells. [d]Inhibition of 100 nM NECA-mediated cAMP accumulation [e]Displacement of specific [^{125}I]AB-MECA binding in membranes obtained from hA_3 AR stably expressed in CHO cells. [f]Data for hA_1, hA_{2A}, and hA_3 taken from ref 29.

events. They are involved in the genesis of inflammatory processes, mediating the release of several inflammatory cytokines from mast cells, airway and bronchial epithelial cells, fibroblasts, smooth cells, intestinal epithelial cells, and monocytes.[8,9] In addition, a role in angiogenesis induction,[10,11] glucose metabolism,[12] and growth and development of some tumors[13] has been suggested. In view of these findings, high-affinity and selective A_{2B} AR antagonists are needed as valuable tools to fully establish their therapeutic potential for the treatment of inflammatory diseases, such as asthma[14−16] and colitis,[17−19] and angiogenic diseases such as diabetic retinopathy and cancer.[20]

dx.doi.org/10.1021/jm201177b | J. Med. Chem. 2012, 55, 1490−1499

Nevertheless, A_{2B} ARs are the most poorly characterized of the four ARs subtypes from a pharmacological point of view due to their general low affinity toward the prototypic standard ligands that are commonly utilized to characterize ARs. In particular, the scarce medicinal chemistry knowledge on the structural requirements crucial for high A_{2B} AR affinity and selectivity raised wide-ranging difficulty in the study of this receptor. However, a number of high-affinity A_{2B} AR antagonists containing different heterocyclic cores have been described which showed various degree of binding selectivity with respect to the other subtypes,[21,22] including deazaxanthines **I**,[23] pyrrolopyrimidines **II**,[24] pyrazolotriazolopyrimidines **III**,[25] and 2-aminopyrimidines **IV**[26,27] (Chart 1).

Over the past decade, we have focused our attention on ARs, disclosing several classes of selective A_1 AR antagonists, including the 3-aryl[1,2,4]triazino[4,3-*a*]benzimidazol-4(10*H*)-ones,[28,29] the *N*-alkyl and *N*-acyl-(7-substituted-2-phenylimidazo[1,2-*a*][1,3,5]triazin-4-yl)amines,[29,30] the 2-(benzimidazol-2-yl)quinoxalines,[31] and selective A_3 AR antagonists, such as the 5-amino-2-phenyl[1,2,3]triazolo[1,2-*a*]-[1,2,4]benzotriazines,[32] the 4-amino-6-hydroxy-2-mercaptopyrimidines,[33] and N^2-substituted-pyrazolo[3,4-*d*]pyrimidines.[34]

In an effort to identify novel ligands possessing high affinity and selectivity for the A_{2B} AR subtype, we further investigated the class of 3-aryl[1,2,4]triazino[4,3-*a*]benzimidazol-4(10*H*)-ones **V** by virtue of their structural similarity with the pyrazolotriazolopyrimidine class **III**. Both series possess a central aromatic tricyclic nitrogen-containing core (6,5,6 for the triazinobenzimidazoles **V** and 5,6,5 for the pyrazolotriazolobenzotriazines **III**) featuring mostly lipophilic substituents and groups able to engage in hydrogen bonds with the receptor protein.

We preliminarily assayed a number of triazinobenzimidazole derivatives derived from our "in-house" collection (compounds **1**−**6**, **9**, and **10**) to define their binding profiles at human A_1, A_{2A}, A_{2B}, and A_3 ARs (Table 1). All the derivatives, with the exception of **6**, showed high affinity at A_{2B} AR (IC_{50} values in the low nanomolar range) with various degrees of selectivity toward A_1 and A_{2A} ARs. These data represented the rationale for the investigation of a series of new derivatives from this class (compounds **7**, **8**, and **11**−**14**), featuring modified substituents at the 10-position (4′-chlorophenyl or phenylethyl groups) and a chlorine atom at the 7-position (X) of the triazinobenzimidazole nucleus, to obtain potent and selective A_{2B} AR antagonists.

The present paper describes the synthesis, the biological evaluation, and the molecular modeling studies of a number of triazinobenzimidazole derivatives **1**−**14** as A_{2B} AR antagonists.

Furthermore, the efficacy of the compounds **1**, **6**−**8**, **11**, **13**, **14** in an in vitro model of experimental colitis was evaluated by assessing their ability to promote the survival of human epithelial colorectal adenocarcinoma cells (Caco-2 cells).[35]

CHEMISTRY

Compounds **1**−**6** and **9**−**10** were synthesized as previously reported.[28,36]

The general synthetic pathway yielding the novel triazinobenzimidazole derivatives **7**, **8**, and **11**−**14** is outlined in Scheme 1, and it proceeded with the conversion of the 2-chlorobenzimidazoles **15**−**17** into the corresponding 2-hydrazones **18**−**20** by reaction with hydrazine hydrate at 180 °C in a Pyrex-capped tube (yield 92−93%). Subsequently, derivatives **18**−**20** and the appropriate aryloxoacetic acid (2-oxo-2-phenylacetic acid, 2-furan-2-yl-2-oxoacetic acid) were allowed to react in refluxing ethanol. In agreement with our previous findings,[28,36] obtaining the target tricyclic compounds **7**, **8**, and **11**−**14** reasonably proceeded through the formation of the intermediate 2-(benzimidazol-2-ylhydrazono)-2-substituted-acetic acids. In fact, in the reaction with the 2-furan-2-yl-2-oxoacetic acid, the acid intermediates **21**−**23** were isolated (Scheme 1) and purified by suspension in hot methanol (yield 65−80%). The best yields (62−67%) in the cyclization process of acids **21**−**23** to the desired derivatives **8**, **12**, and **14** were obtained using one of the following methods: (A) heating the acid **21** at a temperature 30−40 °C above its melting point for 10 min or (B) refluxing the acids **22** and **23** for 1 h in glacial acetic acid (Scheme 1). In the reaction of 2-hydrazinobenzimidazoles **18**−**20** with 2-oxo-2-phenylacetic acid in refluxing ethanol, it was not possible to isolate the intermediate hydrazono derivatives, but the target products **7**, **11**, and **13** were directly obtained (yield 60−65%, Scheme 1).

Scheme 1. Synthesis of Triazinobenzimidazole Derivatives 7, 8, and 11−14[a]

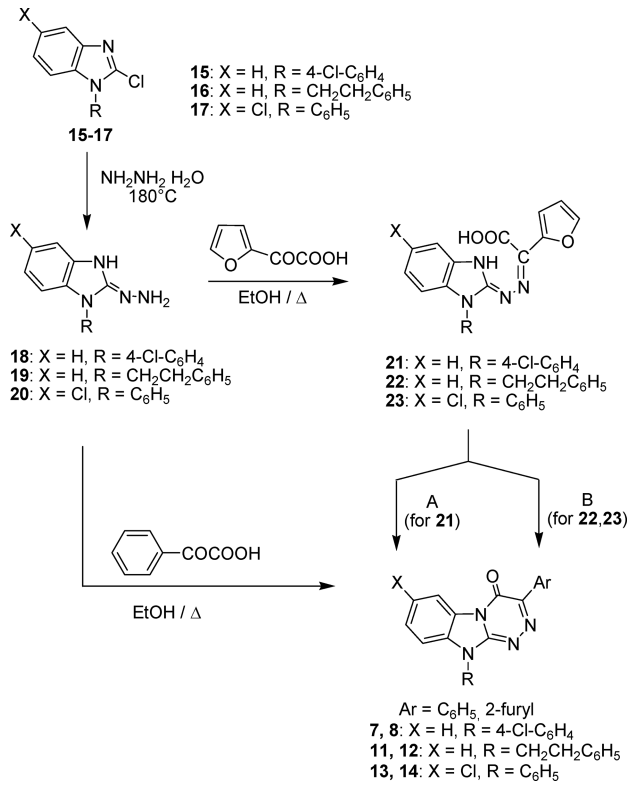

[a]Reagents: (A) heating at 30−40 °C above the melting point; (B) glacial acetic acid, reflux.

The 2-chloro-1-(4-chlorophenyl)-1*H*-benzimidazole **15** and 2,5-dichloro-1-phenyl-1*H*-benzimidazole **17** were easily prepared in two steps starting from the commercially available *N*-(4-chlorophenyl)-1,2-phenylendiamine **24** and the 4-chloro-*N*-phenyl-1,2-phenylendiamine **25**,[37] respectively (Scheme 2). These last two compounds were quantitatively cyclocondensed through a carbonylation reaction that employed triphosgene (bis-trichloromethyl carbonate)[28] to yield the 1-aryl-1,3-dihydro-2*H*-benzimidazol-2-ones **26** and **27** (yield 96−97%). The corresponding 2-chloro derivatives **15** and **17** were obtained by reaction of **26** and **27** with phenylphosphonic dichloride ($PhPOCl_2$) at 170 °C (yield 60−66%).[28]

dx.doi.org/10.1021/jm201177b | J. Med. Chem. 2012, 55, 1490−1499

Scheme 2. Synthesis of 2-Chlorobenzimidazole Derivatives 15 and 17

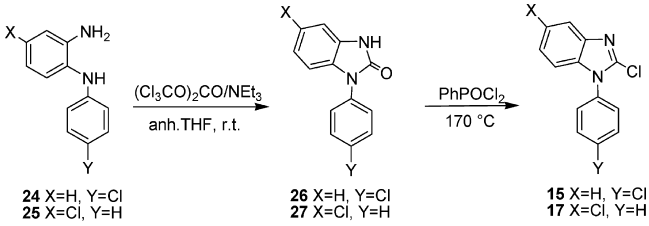

24 X=H, Y=Cl
25 X=Cl, Y=H

26 X=H, Y=Cl
27 X=Cl, Y=H

15 X=H, Y=Cl
17 X=Cl, Y=H

The preparation of the N^1-phenylethyl compound **16** was performed by alkylation of the commercially available 2-chlorobenzimidazole with 2-bromoethylbenzene in the presence of sodium hydride, in accordance with a reported procedure.[38]

BIOLOGY

The affinities of the new compounds toward human A_1, A_{2A}, and A_3 ARs were evaluated by competition experiments assessing their respective abilities to displace [^{3}H]8-cyclopentyl-1,3-dipropylxanthine ([^{3}H]DPCPX), [^{3}H]5′-*N*-ethylcarboxamideadenosine ([^{3}H]NECA), or [^{125}I]4-aminobenzyl-5′-*N*-methylcarboxamidoadenosine ([^{125}I]AB-MECA) binding from transfected CHO cells. The experiments were performed as described elsewhere.[29] Binding affinity at human A_{2B} AR was evaluated in functional assays by measuring the compound's effect on NECA-mediated cAMP accumulation in transfected CHO cells. Finally, selected compounds (**1**, **6**−**8**, **11**, **13**, and **14**) were evaluated in vitro for their ability to modulate the survival of Caco-2 cells by the 3-(4,5-dimethylthiazol-2-yl)-5-(3-carboxymethoxyphenyl)-2-(4-sulfophenyl)-2*H*-tetrazolium (MTS) assay.

RESULTS AND DISCUSSION

The binding data of the triazinobenzimidazole derivatives **1**−**14** at the human A_1, A_{2A}, A_{2B}, and A_3 ARs are summarized in Table 1, together with those of DPCPX, NECA, and Cl-IBMECA reported as reference standards.

From a general point of view, all the reported compounds, with the exception of **6** and **14**, showed affinity at the A_{2B} AR subtype in the nanomolar range (1.40−54.3 nM) with almost complete selectivity toward the A_3 AR and different degrees of selectivity with regard to the A_1 and A_{2A} AR subtypes.

Interestingly, the affinity at the A_{2B} AR is similar for all the derivatives, independent of the nature of the substitution at the 3-, 7-, or 10-positions of the triazinobenzimidazole nucleus. On the contrary, these substitutions seem to significantly modulate the affinity toward the other receptor subtypes, with a consequent influence on selectivity, in an interdependent and not additive way.

In particular, for the major SAR, we can draw concerns on the effect of the aryl group at the 3-position of the triazinobenzimidazole nucleus on A_{2A} AR binding ability. The presence of a pendant 3-phenyl ring seems to be a crucial requirement to gain A_{2B} AR/A_{2A} AR selectivity, as this phenyl hampers the interaction with A_{2A} AR; all the derivatives featuring such a substitution were completely inactive at this latter subtype. In fact, a number of compounds bearing a 2-furyl ring at the 3-position show significant A_{2A} AR affinity with K_i values in the nanomolar range (**2** K_i (hA_{2A}) 33 nM, **8** K_i (hA_{2A}) 50.6 nM, **10** K_i (hA_{2A}) 156 nM, **12** K_i (hA_{2A}) 15.8 nM) and reduced A_{2B}/A_{2A} selectivity. Reasonably, this small five-membered furyl ring might be able to engage positive interactions with an area in the A_{2A} AR site that is not feasible for the phenyl group. In contrast, the A_{2B} AR antagonist binding site could be characterized by lipophilic areas well tolerating both the 2-furyl and phenyl rings.

Stating these considerations, an in-depth analysis of the data reported in Table 1 shows that the affinity and selectivity profile for the ARs within the 3-phenyl and 3-(2-furyl) subseries strictly depends on the substitution at N^{10}.

The 3-(2-furyl)-N^{10}-unsubstituted compound **2** shows comparable affinity at A_1, A_{2A}, and A_{2B} ARs, probably due to the absence of groups able to discriminate between the different binding sites. Insertion at N^{10} of the small lipophilic methyl (**4**), as well as of the phenyl ring (**6**) or benzyl group (**10**), lowers affinity at both A_1 and A_{2A} ARs, suggesting the disruption of an H-bond involving the NH at position 10 or the absence of efficacious lipophilic interactions between these substituents and specific areas of the binding sites. This effect becomes even more evident when a chlorine atom is placed at the 7-position of **6**, yielding derivative **14**, completely inactive at A_1 and A_{2A} ARs. Conversely, substitution at N^{10} with 4-chlorophenyl (**8**) or phenylethyl (**12**) moieties determine a loss in A_1 affinity, with a substantial maintenance of the ability to bind A_{2A} AR, producing quite potent/nonselective A_{2A}/A_{2B} antagonists (**8** K_i (hA_{2A}) 50.6 nM, IC_{50} (hA_{2B}) 2.11 nM; **12** K_i (hA_{2A}) 15.8 nM, IC_{50} (hA_{2B}) 5.34 nM).

Concerning the subset of 3-phenyl-substituted derivatives, the lack of substitution at N^{10} in compound **1** afforded a very good A_{2B}/A_1 selectivity, with **1** as an excellent performing derivative in terms of A_{2B} affinity and selectivity (K_i (hA_1) 728 nM, K_i (hA_{2A}) > 10000 nM, IC_{50} (hA_{2B}) 1.40 nM, K_i (hA_3) > 1000 nM). Insertion of a methyl, phenyl, or benzyl group (**3**, **5**, and **9**, respectively) generally increases A_1 AR affinity and maintains A_{2B} AR affinity in the nanomolar range, thus reducing A_{2B}/A_1 selectivity. Insertion of a chlorine at the 4-position of the N^{10}-phenyl ring of **5** (**7**), as well as homologation of the N^{10}-benzyl group of **9** to a 2-phenylethyl chain (**11**), causes a loss in A_1 AR affinity while maintaining high A_{2B} AR affinity (**7** K_i (hA_1) 1357 nM, IC_{50} (hA_{2B}) 2.42 nM; **11** K_i (hA_1) > 10000 nM, IC_{50} (hA_{2B}) 2.50 nM). Taken together, these data suggest that the lipophilic area hosting the N^{10}-substituent in the A_{2B} AR is more tolerant with respect to the corresponding pocket in the A_1 AR binding site.

Finally, insertion of a chlorine at the 7-position of the triazinobenzimidazole nucleus of **5** produces derivative **13**, which is the most potent and selective of all the compounds investigated, with a IC_{50} of 3.10 nM at A_{2B} AR and no activity at A_1, A_{2A}, and A_3 ARs. The same substitution pattern on the furyl derivative **6** yields derivative **14**, showing no activity at all AR subtypes.

Compounds **1**, **7**, **8**, **11**, and **13** were selected and tested in vitro for their ability to modulate the survival of Caco-2 cells. A_{2B} AR is the subtype predominantly expressed in these cultured human epithelia cells widely used as an in vitro model of experimental colitis. Cell treatment for 24 h with the nonselective AR agonist, NECA (100 nM), induced a significant decrease in cell viability with respect to untreated control cells. To evaluate if NECA-induced toxicity could be reversed by A_{2B} AR antagonists, Caco-2 cells were incubated with different concentrations of **1**, **7**, **8**, **11**, and **13** (ranging from 0.1 to 50 nM), either in the absence or presence of 100 nM NECA for 24 h. The results show that the compounds

dx.doi.org/10.1021/jm201177b | *J. Med. Chem.* 2012, 55, 1490−1499

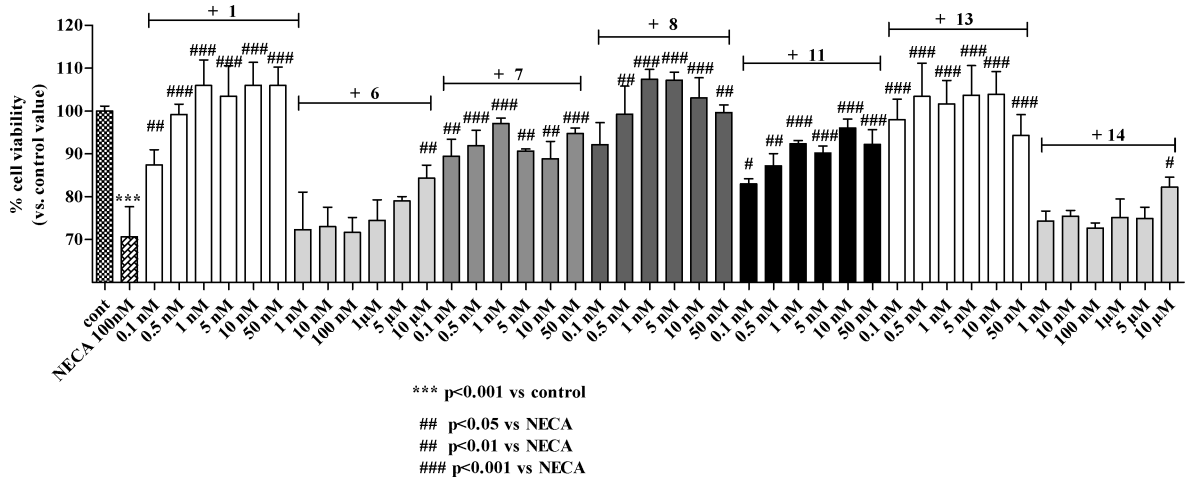

Figure 1. Effect of A_{2B} AR antagonists on Caco-2 cell survival. Cells were treated for 24 h with 100 nM NECA in the absence or in the presence of different compound concentrations. Following incubation, cell survival was quantified by MTS assay as described in Experimental Section. Data are expressed as percentage of control value (set to 100%) and represent the mean ± SEM of three different experiments. *** $P < 0.001$ vs control; # $P < 0.05$, ## $P < 0.01$, ### $P < 0.001$ vs NECA alone.

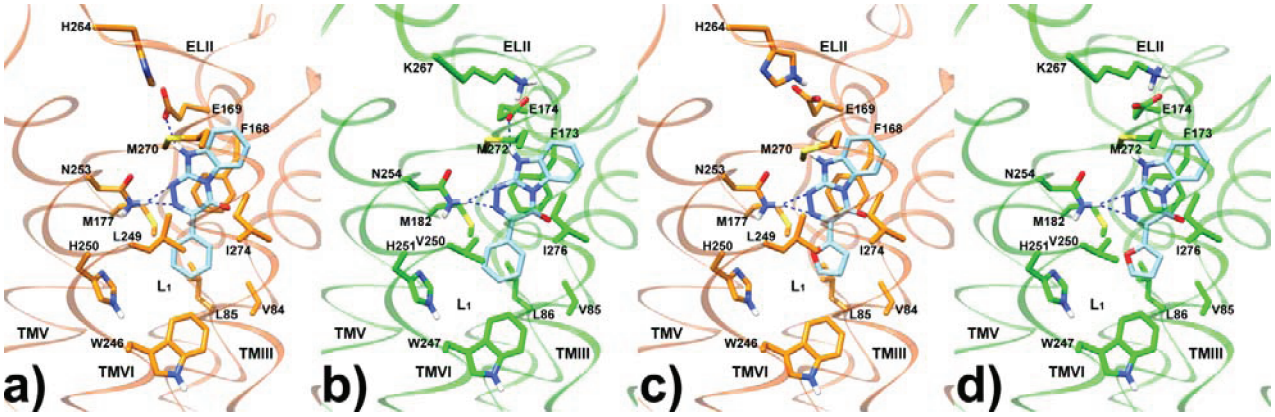

Figure 2. Binding conformation of **1** (a,b) and **2** (c,d) in A_{2A} AR (a,c) and A_{2B} AR (b,d) as calculated by Glide. The receptor is represented as orange (A_{2A} AR) and green (A_{2B} AR) sticks and ribbons. The ligand is represented as cyan sticks, while H-bonds are represented as blue dashed lines. For sake of clarity, only interacting residues are shown.

alone were unable to induce any significant effect on cell viability (data not shown). In the presence of NECA, all the A_{2B} AR antagonists significantly reversed NECA-induced cell death at all tested concentrations (Figure 1); these effects were detectable at nanomolar compound concentrations, comparable to IC_{50} values of each compound toward A_{2B} ARs. To confirm that the observed cellular effects were derived from the selective A_{2B} AR antagonism, the same experiments were performed using compounds **6** and **14** as negative controls. The data depicted in Figure 1 show that these compounds were able to revert NECA-induced cell death only at the highest concentration used based on their low affinity for A_{2B} AR subtype. The results suggest that these A_{2B} AR antagonists act as pro-survival agents in protecting Caco-2 cells by death induced by the AR agonist NECA and may provide the basis for the development of potential adjuvant agents in the treatment of colitis.

MOLECULAR MODELING

To better understand the reasons behind the selective binding of the newly discovered AR ligands, molecular modeling studies were undertaken starting from the recently published 2.6 Å crystal structure of A_{2A} AR (PDB code 3EML) in complex with compound ZM241385.[39] This study by Stevens and co-workers demonstrated that the A_{2A} AR structure shares an overall seven transmembrane (TM) helix architecture similar to that of the rhodopsin and adrenergic receptors, with small differences residing in the positions and orientations of the helices. Conversely, larger structural differences were recorded in the extracellular loops and, most of all, in the ligand orientation. Indeed, if compared with the β-adrenergic ligands and retinal, ZM241385 in the A_{2A} AR occupies a significantly different position in the transmembrane (TM) bundle, being almost parallel to the receptor axis. This orientation allows the bicyclic triazolotriazine core of the antagonist to establish favorable interactions with the F168, I274, N253, and E169 residues.

The above-described structure was used to obtain a homology model of the hA_{2B} ARs. The sequence alignment between the receptors as well as the positions of the disulfide bridges we obtained are consistent with what has already been suggested by Moro and co-workers (see Figure S1 in Supporting Information).[40] Then, the structures of the modeled receptors were used to dock the highly affine and selective 3-phenyl derivative **1** and its fur-2-yl analogue **2**, which is instead unselective for the four ARs. These calculations were obtained with the Glide program of the Schrodinger package,

dx.doi.org/10.1021/jm201177b | J. Med. Chem. 2012, 55, 1490–1499

which has already been used to successfully dock a series of ARs antagonists.[41] Interestingly, in the inspected compounds, the simple substitution of a furyl ring (**2**) with a phenyl one (**1**) completely abolishes the affinity for the A_{2A} AR while maintaining low nanomolar affinities at the A_{2B} AR. Thus, as a first step, we decided to analyze the docking results obtained in these two receptors. Unexpectedly, in the Glide results, the same well-defined binding pose was found for the four dockings. As shown in Figure 2, compounds **1** and **2** are both capable of placing their triazinobenzimidazole ring on the outer portion of the A_{2A} and A_{2B} ARs, surrounded by TMs III, V, VI, VII helices, and ELII.

Such a position allows H-bond interactions with the N253 and N254 of the A_{2A} and A_{2B} ARs, respectively. These interactions seem to be critical for antagonist affinity, as underscored by X-ray crystallography[39] and mutagenesis data demonstrating that the sole substitution of the aforementioned asparagine with an alanine results in the complete loss of antagonist radioligands binding.[42] Moreover, compounds **1** and **2**, with their imidazole NH group, H-bond with E169(A_{2A}) and E174(A_{2B}). These favorable contacts anchor the phenyl and furyl rings of **1** and **2** in a hydrophobic cleft (herein referred as L_1) made up by V84, L85, M177, W246, P248, L249, and H250 in the A_{2A}AR and by V85, L86, M182, W247, P249, V250, and H251 in the A_{2B}AR, respectively. Previous studies[39,43,44] and the very recent pioneering work by Stevens and co-workers[45] have revealed several residues lining the L_1 pocket to be responsible for A_{2A} AR activation. In particular, comparison between the agonist- and antagonist-bound X-ray structures have revealed that W246 and H250 respectively experience 1.9 and ∼1.8 Å movements to adapt to the bound ligand. These modest local rearrangements trigger major movements in the receptor helical bundle. Thus, the favorable van der Waals contacts between the ligand furyl and phenyl rings and these residues might prevent the structural rearrangements responsible for the activation, constraining the receptors in an inactive state. Additionally, in the four calculated complexes, the triazinobenzimidazolone scaffold is stably anchored to the receptor through a π-stacking interaction with F168(A_{2A}) and F173(A_{2B}) of ELII.

In contrast to compounds **1** and **2**, compounds **3**−**14** bear a substituent at the imidazole nitrogen, and such a feature prevents these ligands from adopting the same binding pose observed for the unsubstituted analogues. In fact, docking of compound **11** in A_{2B} AR resulted in a new binding pose where the phenyl ring is still placed in the L_1 pocket, whereas the triazinobenzimidazole scaffold H-bonds N254 through its carbonyl oxygen in position 4 (Figure 3). This change in the heterocyclic orientation prevents the steric clash with E174(A_{2B}) and orients the phenylethyl pendant chain toward a rather lipophilic cleft, made up by I67, A64, F63, and V85, at the crevice between TMII and TMIII. By featuring the interaction with the critical N254 and L_1 pocket, the different binding pose would still allow **11** to be as equipotent and selective as **1**.

Unfortunately, the above-described theoretical results somehow disagree with the observed experimental data suggesting a high binding of **1** at the A_{2B} AR, whereas no binding was detected at the A_{2A} AR. To overcome the intrinsic limitations of docking algorithms (i.e., absence of receptor flexibility), preliminary molecular dynamics simulations were performed (see Supporting Information for details). These findings allowed us to speculate that the residue composition of the

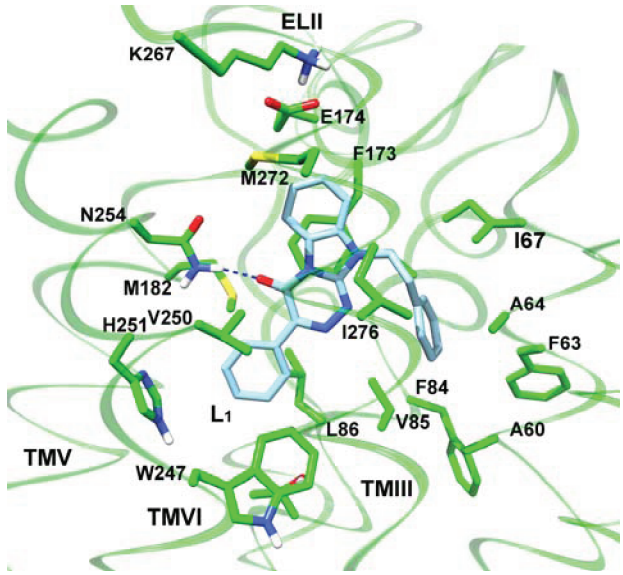

Figure 3. Binding conformation of **11** in the A_{2B}AR as calculated by Glide. The receptor is represented as green sticks and ribbons. The ligand is represented as cyan sticks, while H-bonds are represented as blue dashed lines. For sake of clarity, only interacting residues are shown.

L_1 pocket in the two receptors (A_{2A} and A_{2B} ARs) might deeply influence the dynamical stabilization of the aforementioned binding modes, thus explaining the recorded selectivity profiles. Interestingly, the same conclusions have also been drawn by other authors.[46,47]

CONCLUSIONS

A novel class of high affinity and selectivity A_{2B} AR ligands featuring the 3-aryl[1,2,4]triazino[4,3-*a*]benzimidazol-4(10*H*)-one as the core scaffold has been developed. The majority of the compounds show good to high A_{2B} AR affinity and are completely inactive and moderately active at A_3 and A_1 ARs, respectively, whereas the A_{2B} AR/A_{2A} AR selectivity is strictly dependent on the aryl group at the 3-position of the central core. Specifically, as rationalized by molecular modeling studies, the presence of a pendant 3-phenyl ring appears to hamper the interaction with A_{2A} AR, conferring high A_{2B}/A_{2A} AR selectivity.

Finally, selected compounds **1**, **7**, **8**, **11**, and **13**, when tested in vitro in a widely used model of experimental colitis, significantly reversed NECA-induced cell death at nanomolar compound concentrations relative to their A_{2B} AR IC_{50} values, acting as pro-survival agents and providing the basis for the development of potential adjuvant agents in the treatment of colitis.

EXPERIMENTAL SECTION

Chemistry. Melting points were determined using a Reichert Köfler hot-stage apparatus and are uncorrected. Infrared spectra were recorded with a Nicolet/Avatar FT-IR spectrometer in Nujol mulls. Routine nuclear magnetic resonance spectra were recorded in DMSO-d_6 solution on a Varian Gemini 200 spectrometer operating at 200 MHz. Evaporation was performed in vacuo (rotary evaporator). Analytical TLC was carried out on Merck 0.2 mm precoated silica gel aluminum sheets (60 F-254). Combustion analyses on target compounds were performed by our Analytical Laboratory in Pisa. All compounds showed ≥95% purity.

2-Chlorobenzimidazole, 2-phenylethyl bromide, *N*-(4-chlorophenyl)-1,2-phenylendiamine **24**, triphosgene (bis-trichloromethyl carbo-

dx.doi.org/10.1021/jm201177b | *J. Med. Chem.* 2012, 55, 1490−1499

nate), and phenylphosphonic dichloride ($PhPOCl_2$) were from Sigma-Aldrich. The following compounds were prepared in accordance with reported procedures: 3-phenyl[1,2,4]triazino[4,3-*a*]benzimidazol-4-(10*H*)-one **1**,[36] 3-(2-furyl)[1,2,4]triazino[4,3-*a*]benzimidazol-4-(10*H*)-one **2**,[36] 10-methyl-3-phenyl[1,2,4]triazino[4,3-*a*]-benzimidazol-4(10*H*)-one **3**,[36] 3-(2-furyl)-10-methyl[1,2,4]triazino-[4,3-*a*]benzimidazol-4(10*H*)-one **4**,[36] 3,10-diphenyl[1,2,4]triazino[4,3-*a*]benzimidazol-4(10*H*)-one **5**,[28] 3-(2-furyl)-10-phenyl-[1,2,4]triazino[4,3-*a*]benzimidazol-4(10*H*)-one **6**,[28] 10-benzyl-3-phenyl[1,2,4]triazino[4,3-*a*]benzimidazol-4(10*H*)-one **9**,[28] 10-benzyl-3-(2-furyl)[1,2,4]triazino[4,3-*a*]benzimidazol-4(10*H*)-one **10**,[28] 2-chloro-1-(2-phenylethyl)benzimidazole **16**,[38,48] and 4-chloro-*N*-phenyl-1,2-phenylendiamine **25**.[37]

*General Procedure for the Synthesis of 3-Phenyl-5-substituted-10-(substituted-phenyl)[1,2,4]triazino[4,3-a]benzimidazol-4(10H)-ones **7**, **11**, and **13**.* A solution of the appropriate 2-hydrazinobenzimidazole **18**–**20** (4 mmol) and phenyloxoacetic acid (0.660 g, 4.4 mmol) in 10 mL of absolute ethanol was refluxed for 5 h (TLC analysis). After cooling, the precipitate which formed was collected and purified by crystallization from the appropriate solvent.

*10-(4-Chlorophenyl)-3-phenyl[1,2,4]triazino[4,3-a]benzimidazol-4(10H)-one **7**.* Yield 65%; mp = 225–227 °C (EtOH). IR (nujol, cm^{-1}): 1680, 1600, 1300, 1150, 760. ^1H NMR (DMSO-d_6, ppm): 7.43–7.83 (m, 10H), 8.19–8.24 (AA′ part of AA′BB′C system, 2H), 8.61 (pd, 1H). Anal. Calcd for C, H, N.

*3-Phenyl-10-(2-phenylethyl)[1,2,4]triazino[4,3-a]benzimidazol-4(10H)-one **11**.* Yield 60%; mp = 228–230 °C (DMF). IR (nujol, cm^{-1}): 1680, 1570, 1460, 1150, 750. ^1H NMR (DMSO-d_6, ppm): 3.20 (t, 2H, J = 7.3 Hz), 4.65 (t, 2H, J = 7.3 Hz), 7.16–7.33 (m, 5H), 7.38–7.68 (m, 6H), 8.18–8.24 (AA′ part of AA′BB′C system, 2H), 8.48 (pd, 1H). Anal. Calcd for C, H, N.

*7-Chloro-3,10-diphenyl[1,2,4]triazino[4,3-a]benzimidazol-4(10H)-one **13**.* Yield 65%; mp = 248–250 °C (EtOH). IR (nujol, cm^{-1}): 1680, 1590, 1550, 1280, 1170, 770. ^1H NMR (DMSO-d_6, ppm): 7.45–7.53 (m, 4H), 7.64–7.80 (m, 6H), 8.12–8.22 (AA′ part of AA′BB′C system, 2H), 8.57 ppm (ps, 1H). Anal. Calcd for C, H, N.

*General Procedure for the Synthesis of 3-(2-Furyl)-10-(substituted-phenyl)[1,2,4]triazino[4,3-a]benzimidazol-4(10H)ones **8**, **12**, and **14**.* The appropriate (1,5-disubstituted-benzimidazol-2-ylhydrazono)substituted-acetic acids **21**–**23** were cyclized by means of the following methods.

Method A. The acid derivative **21** (2 mmol) was heated at a temperature 30–40 °C above its melting point for 10 min, so that thermal cyclization occurred. After cooling, product **8** was purified by recrystallization from EtOH.

Method B. A suspension of the acid derivatives **22**, **23** (2 mmol) in 20 mL of glacial acetic acid was refluxed for 1 h. The solution obtained was evaporated to dryness, and the oily residue was purified by recrystallization from EtOH.

*10-(4-Chlorophenyl)-3-(2-furyl)[1,2,4]triazino[4,3-a]-benzimidazol-4(10H)-one **8**.* Method A. Yield 67%; mp = 233–235 °C. IR (nujol, cm^{-1}): 1685, 1600, 1560, 1260, 1100, 760. ^1H NMR (DMSO-d_6, ppm): 6.72 (dd, 1H, J = 3.4, J = 1.8 Hz), 7.47–7.68 (m, 5H), 7.81–7.85 (m, 3H), 7.92 (dd, 1H, J = 1.8, J = 0.9 Hz), 8.59 (pd, 1H). Anal. Calcd for C, H, N.

*3-(2-Furyl)-10-(2-phenylethyl)[1,2,4]triazino[4,3-a]benzimidazol-4(10H)-one **12**.* Method B. Yield 62%; mp = 190–192 °C. IR (nujol, cm^{-1}): 1675, 1560, 1480, 1150, 750. ^1H NMR (DMSO-d_6, ppm): 3.19 (t, 2H, J = 7.3 Hz), 4.65 (t, 2H, J = 7.3 Hz), 6.69–6.72 (m, 1H), 7.14–7.30 (m, 5H), 7.37–7.45 (m, 2H), 7.53–7.67 (m, 2H), 7.90–7.91 (m, 1H), 8.47 (pd, 1H). Anal. Calcd for C, H, N.

*7-Chloro-3-(2-furyl)-10-phenyl[1,2,4]triazino[4,3-a]benzimidazol-4(10H)-one **14**.* Method B. Yield 66%; mp = 252–254 °C. IR (nujol, cm^{-1}): 1680, 1570, 1520, 1280, 1190, 770. ^1H NMR (DMSO-d_6, ppm): 6.76 (dd, 1H, J = 3.5, J = 1.8 Hz), 7.44–7.50 (m, 3H), 7.60–7.68 (m, 5H), 7.97–7.98 (m, 1H), 8.57 (ps, 1H). Anal. Calcd for C, H, N.

*General Procedure for the Synthesis of 2-Chloro-5-substituted-1-(4-substituted-phenyl)benzimidazole **15** and **17**.* A mixture of the appropriate benzimidazole derivative **26** and **27** (6.0 mmol) and 14.0 mL of $PhPOCl_2$ was heated at 170 °C for 19 h (TLC analysis), under stirring and with exclusion of moisture. After cooling, the excess reagent was decomposed by addition of ice and water; the obtained aqueous suspension was neutralized with conc NH_4OH, after which the desired products **15** and **17** were isolated directly in a pure state by filtration.

*2-Chloro-1-(4-chlorophenyl)-1H-benzimidazole **15**.* Yield 66%; mp: 128–130 °C (lit.[49] mp = 132–133 °C). IR (nujol, cm^{-1}): 1590, 1500, 1030, 700. ^1H NMR (DMSO-d_6, ppm): 7.19–7.22 (m, 1H), 7.29–7.34 (m, 2H), 7.64–7.76 (m, 5H). Anal. Calcd for C, H, N.

*2,5-Dichloro-1-phenyl-1H-benzimidazole **17**.* Yield 60%; mp: 105–107 °C. IR (nujol, cm^{-1}): 1590, 1500, 1050, 760. ^1H NMR (DMSO-d_6, ppm): 7.15–7.40 (AB part of ABX system, 2H), 7.63–7.66 (m, 5H), 7.81–7.83 (X part of ABX system, 1H). Anal. Calcd for C, H, N.

*General Procedure for the Synthesis of 1-Substituted-1,3-dihydro-2H-benzimidazol-2-one hydrazones **18**–**20**.* The appropriate substituted-2-chlorobenzimidazole **15**–**17** (2.7 mmol) was heated at 180 °C in a Pyrex capped tube with 1.0 mL of hydrazine monohydrate for 5 h. After the mixture was cooled, a white solid separated, which was collected and resulted sufficiently pure to be used in the next reaction without further purification.

*1-(4-Chlorophenyl)-1,3-dihydro-2H-benzimidazol-2-one hydrazone **18**.* Yield 92%; mp = 115–117 °C. IR (nujol, cm^{-1}): 3250–2700, 1650, 1610, 1090, 830. ^1H NMR (DMSO-d_6, ppm): 6.94–7.08 (m, 3H), 7.33–7.68 (m, 5H). Anal. Calcd for C, H, N.

*1-(2-Phenylethyl)-1,3-dihydro-2H-benzimidazol-2-one hydrazone **19**.* Yield 92%; mp = 99–101 °C. IR (nujol, cm^{-1}): 3500–2650, 1620, 1600, 1560, 1140, 740. ^1H NMR (DMSO-d_6, ppm): 3.12 (t, 2H, J = 7.3 Hz), 4.50 (t, 2H, J = 7.3 Hz), 7.03–7.46 (m, 7H), 7.60–7.64 (m, 2H). Anal. Calcd for C, H, N.

*5-Chloro-1-phenyl-1,3-dihydro-2H-benzimidazol-2-one hydrazone **20**.* Yield 93%; mp = 109–111 °C. IR (nujol, cm^{-1}): 3340–2875, 1620, 1300, 1160, 790. ^1H NMR (DMSO-d_6, ppm): 6.87–7.12 (m, 3H), 7.35–7.68 (m, 5H). Anal. Calcd for C, H, N.

*General Procedure for the Synthesis of (1,5-Disubstituted-benzimidazol-2-ylhydrazono)-(2-furyl)acetic Acids **21**–**23**.* A solution of the appropriate benzimidazol-2-one hydrazones **18**–**20** (4 mmol) and the 2-furyloxoacetic acid (0.616 g, 4.4 mmol) in 10 mL of absolute ethanol was refluxed for 2 h. After cooling, the precipitate which formed was collected to give the substituted (benzimidazol-2-ylhydrazono)acetic acids **21**–**23** which were purified by suspension in hot methanol.

*{[1-(4-Chlorophenyl)-1,3-dihydro-2H-benzimidazol-2-ylidene]-hydrazono}-(2-furyl)acetic Acid **21**.* Yield 76%; mp = 128–131 °C. IR (nujol, cm^{-1}): 3500–2800, 1600, 1380, 1020, 720. ^1H NMR (DMSO-d_6, ppm): 6.61 (dd, 1H, J = 3.4, J = 1.7 Hz), 7.09–7.18 (m, 4H), 7.23–7.46 (m, 1H), 7.73–7.79 (m, 5H), 12.60 (bs, 1H). Anal. Calcd for C, H, N.

*2-Furyl-{[1-(2-phenylethyl)-1,3-dihydro-2H-benzimidazol-2-ylidene]hydrazono}acetic Acid **22**.* Yield 65%; mp = 202–204 °C. IR (nujol, cm^{-1}): 3200–2800, 1650, 1620, 1280, 1140, 740. ^1H NMR (DMSO-d_6, ppm): 3.06 (t, 2H, J = 7.6 Hz), 4.29 (t, 2H, J = 7.6 Hz), 6.61 (dd, 1H, J = 3.3, J = 1.8 Hz), 7.16–7.49 (m, 10H), 7.77–7.79 (m, 1H), 12.34 (bs, 1H). Anal. Calcd for C, H, N.

*(5-Chloro-1-phenyl-1,3-dihydro-2H-benzimidazol-2-ylidenehydrazono)(2-furyl)acetic Acid **23**.* Yield 80%; mp = 186–189 °C. IR (nujol, cm^{-1}): 3500–2500, 1660, 1590, 1305, 1120, 790. ^1H NMR (DMSO-d_6, ppm): 6.60–6.62 (m, 1H), 7.06–7.19 (m, 3H), 7.33–7.41 (m, 1H), 7.57–7.81 (m, 5H), 12.27 (bs, 1H). Anal. Calcd for C, H, N.

*General Procedure for the Synthesis of 5-Substituted-1-(4-substituted-phenyl)benzimidazol-2-ones **26** and **27**.* Triphosgene (bis-trichloromethylcarbonate) (1.48 g, 5.0 mmol) was added portionwise, under a nitrogen atmosphere, to an ice-cooled solution of the appropriate 1,2-phenylendiamine **24**, **25** (5.0 mmol) in 47 mL of anhydrous THF. Then a solution of triethylamine (1.7 mL, 12 mmol) in 13 mL of the same solvent was added dropwise, and the reaction mixture was maintained under stirring at 0 °C for 1 h and at room temperature until the disappearance of the starting material (24 h, TLC analysis). The suspension obtained was filtered and the solvent evaporated at reduced pressure, yielding the crude benzimidazolone

derivative **26** and **27**, which was purified by crystallization from toluene.

1-(4-Chlorophenyl)-1,3-dihydro-2H-benzimidazol-2-one ***26***. Yield 98%; mp: 211−212 °C (lit.[50] mp = 206−208 °C). Anal. Calcd for C, H, N.

5-Chloro-1-phenyl-1,3-dihydro-2H-benzimidazol-2-one ***27***. Yield 97%; mp: 228−230 °C (lit.[51] mp = 222−223 °C). Anal. Calcd for C, H, N.

Biology. *Adenosine Receptor Binding Assay. Materials.* [^{3}H]DPCPX, [^{3}H]NECA, and [^{125}I]AB-MECA were obtained from DuPont-NEN (Boston, MA). ADA was from Sigma Chemical Co. (St. Louis, MO). All other reagents were from standard commercial sources and of the highest commercially available grade. CHO cells stably expressing human A_1, A_{2A}, and A_3 ARs were kindly supplied by Prof. K. N. Klotz, Wurzburg University, Germany.[52]

Human A_1 Adenosine Receptors. Aliquots of membranes (50 μg proteins) obtained from A_1 CHO cells were incubated at 25 °C for 180 min in 500 μL of T_1 buffer (50 mM Tris-HCl, 2 mM $MgCl_2$, 2 units/mL ADA, pH 7.4) containing [^{3}H]DPCPX (3 nM) and six different concentrations of the newly synthesized compounds. Nonspecific binding was determined in the presence of 50 μM R-PIA.[29] The dissociation constant (K_d) of [^{3}H]DPCPX in A_1 CHO cell membranes was 3 nM.

Human A_{2A} Adenosine Receptors. Aliquots of cell membranes (80 μg) were incubated at 25 °C for 90 min in 500 μL of T_2 buffer (50 mM Tris-HCl, 2 mM $MgCl_2$, 2 units/mL ADA, pH 7.4) in the presence of 30 nM of [^{3}H]NECA and six different concentrations of the newly synthesized compounds. Nonspecific binding was determined in the presence of 100 μM NECA.[29] The dissociation constant (K_d) of [^{3}H]NECA in A_{2A} CHO cell membranes was 30 nM.

Human A_3 Adenosine Receptors. Aliquots of cell membranes (40 μg) were incubated at 25 °C for 90 min in 100 μL of T_3 buffer (50 mM Tris-HCl, 10 mM $MgCl_2$, 1 mM EDTA, 2 units/mL ADA, pH 7.4) in the presence of 1.4 nM [^{125}I]ABMECA and six different concentrations of the newly synthesized compounds. Nonspecific binding was determined in the presence of 50 μM R-PIA.[29] The dissociation constant (K_d) of [^{125}I]AB-MECA in A_3 CHO cell membranes was 1.4 nM.

All compounds were routinely dissolved in DMSO and diluted with assay buffer to the final concentration, where the amount of DMSO never exceeded 2%. Percentage inhibition values of specific radiolabeled ligand binding at 1−10 μM concentration are means ± SEM of at least three determinations. For compound IC_{50} determination, at least six different ligand concentrations were used. IC_{50} values, computer-generated using a nonlinear regression formula on a computer program (Graph-Pad, San Diego, CA), were converted to K_i values, based on the K_d values of radioligands in the different tissues and using the Cheng and Prusoff equation.[53] K_i values are means ± SEM of at least three determinations.

Measurement of Cyclic AMP Levels on hA_{2B} CHO Cells. Intracellular cyclic AMP (cAMP) levels were measured using a competitive protein binding method.[54] CHO cells, expressing recombinant hA_{2B} ARs, were harvested by trypsinization. After centrifugation and resuspension in medium, cells (~48000) were plated in 24-well plates in 0.5 mL of medium. After 48 h, the medium was removed, and the cells were incubated at 37 °C for 15 min with 0.5 mL of Dulbecco's Modified Eagle Medium (DMEM) in the presence of adenosine deaminase (1U/mL) and the phosphodiesterase inhibitor Ro20-1724 (20 μM). The antagonism profile of the new compounds toward A_{2B} AR was evaluated by assessing their ability to inhibit 100 nM NECA-mediated accumulation of cAMP. Cells were incubated in the reaction medium (15 min at 37 °C) with different concentrations of the target compound (1 nM to 10 μM) and then were treated with NECA. The reaction was terminated by the removal of the medium and the addition of 0.4 N HCl. After 30 min, lysates were neutralized with 4 N KOH, and the suspension was centrifuged at 800*g* for 5 min. For the determination of cAMP production, bovine adrenal cAMP binding protein was incubated with [^{3}H]cAMP (2 nM) and 50 μL of cell lysate or cAMP standard (0−16 pmol) at 0 °C for 150 min in a total volume of 300 μL. Bound radioactivity was separated by rapid filtration through GF/C glass fiber filters and washed twice with 4 mL of 50 mM Tris/HCl, pH 7.4. The radioactivity was measured by liquid scintillation spectrometry.

Effect of A_{2B} AR Antagonists on Caco-2 Cell Survival. Caco-2 cells were maintained in DMEM medium supplemented with 10% fetal bovine serum, 2 mM L-glutamine, and penicillin/streptomycin in humidified atmosphere (5% CO_2) at 37 °C. Cells were seeded in 96-well microplates (5000 cells/well); the day after, cells were incubated with 100 nM NECA, in the absence or in the presence of A_{2B} AR antagonists, for 24 h. The A_{2B} AR antagonists were added for 5 min prior to addition of NECA in order to determine the inhibition of NECA-mediated cell toxicity. Following incubation times, cell viability was determined using the MTS assay according to manufacturer's instruction. The dehydrogenase activity in active mitochondria reduces MTS to the soluble formazan product. The absorbance of formazan at 490 nM was measured in a colorimetric assay with an automated plate reader.

Data Analysis. Within an experiment, each condition was assayed in duplicate or triplicate, and each experiment was performed at least three times. The results were calculated by subtracting the mean background from the values obtained from each test condition and were expressed as the percentage of the control (untreated cells). Student's *t*-test was used to evaluate whether differences between the experimental groups and the control were statistically significant.

Computational Methods. *Homology Modeling.* hA_{2A} AR structure was downloaded from the Protein Data Bank (PDB code 3EML), and hydrogens were added to the protein and ligand (ZM 241385) using the MOLPROBITY server.[55] Then, the homology model of the hA_{2B}AR was built using Schrödinger Prime[56] software accessible through the Maestro interface.[57] Unless otherwise stated, default parameters were used throughout. The sequences of the hA_1 (P30542), hA_{2B} (P29275), and hA_3 (P33765) ARs were aligned against the sequence of hA_{2A} AR (P29274). Alignment of anchor residues within each TM domain were attained according to the sequence alignment suggested by Moro and co-workers (see Figure S1 in Supporting Information).[40]

During the homology model building, Prime keeps the backbone rigid for the cases in which the backbone does not need to be reconstructed due to gaps in the alignment. The loop refinements were carried out using Prime with default parameter settings, if not mentioned otherwise. Prior to refinement, the protein structures were subjected to a protein preparation step to reorientate side chain hydroxyl groups and alleviate potential steric clashes. The implemented loop modeling protocol consists of several steps.[58] First, large numbers of loops are created by a conformational search in dihedral angle space. Clustering of loop conformations and side chain optimization is being used to select representative solutions. On the basis of the user parameters, a limited number of structures is then processed using complete energy minimization. The top ranked solution in terms of Prime energy was considered best. The short loops (ELI and ELIII) were refined using default sampling rates in the initial step, while the extended, highest sampling rate was chosen for the larger amino acid loops (ELII). Side chains were unfrozen within 7.5 Å of the corresponding loop, and the energy cutoff was set to 10 kcal.

Molecular Docking. The three-dimensional (3D) structures of compounds **1**, **2**, and **11** were drawn using the Builder tool and generated with Ligprep module. The Glide program of the Schrodinger package was used to dock these compounds **1**, **2**, and **11** to the hA_{2A} and hA_{2B} ARs structures. The receptor grid generation were performed for the box with a center in the putative binding site. The size of the box was determined automatically. The extra precision mode (XP) of Glide was used for the docking. The ligand scaling factor was set to 1.0. The geometry of the ligand binding site of the complex between the selected ligands and the four receptors was then optimized. The binding site was defined as the ligand and all amino acid residues located within 8 Å from the ligand. All the receptor residues located within 2 Å from the binding site were used as a shell.

The following parameters of energy minimization were used: OPLS2005 force field; water was used as an implicit solvent; a maximum of 5000 iterations of the Polak−Ribier conjugate gradient minimization method was used with a convergence threshold of 0.01 kJ 3 mol^{-1} $Å^{-1}$.

■ ASSOCIATED CONTENT

Supporting Information

Additional molecular modeling details and figures, analytical data of compounds **7**, **8**, **11**−**15**, **17**−**23**, **26**, and **27**. This material is available free of charge via the Internet at http://pubs.acs.org.

■ AUTHOR INFORMATION

Corresponding Author

*Phone: (+39)0502219547. Fax: (+39)0502219605. E-mail: taliani@farm.unipi.it.

■ ACKNOWLEDGMENTS

This work was financially supported by MIUR (PRIN 2008). We thank Prof. Karl-Norbert Klotz for his generous gift of transfected CHO cells expressing the human A_1, A_{2A}, and A_3 receptors.

■ ABBREVIATIONS USED

AR, adenosine receptor; AB-MECA, 4-aminobenzyl-5′-*N*-methyl-carboxamidoadenosine; CNS, central nervous system; DMEM, Dulbecco's Modified Eagle Medium; DPCPX, 8-cyclopentyl-1,3-dipropylxanthine; GPCRs, G-protein coupled receptors; MTS, 3-(4,5-dimethylthiazol-2-yl)-5-(3-carboxymethoxyphenyl)-2-(4-sulfophenyl)-2*H*-tetrazolium; NECA, 5′-(*N*-ethylcarboxamide)adenosine; R-PIA, N^6-(*R*)-phenylisopropyladenosine; SEM, standard error of mean

■ REFERENCES

(1) Poulsen, S. A.; Quinn, R. J. Adenosine receptors: new opportunities for future drugs. *Bioorg. Med. Chem.* **1998**, *6*, 619−641.
(2) Fredholm, B. B.; Arslan, G.; Halldner, L.; Kull, B.; Schulte, G.; Wasserman, W. Structure and function of adenosine receptors and their genes. *Naunyn Schmiedeberg's Arch. Pharmacol.* **2000**, *362*, 364−374.
(3) Fredholm, B. B.; IJzerman., A. P.; Jacobson, K. A.; Klotz, K.-N.; Linden, J. International Union of Pharmacology. XXV. Nomenclature and classification of adenosine receptors. *Pharmacol. Rev.* **2001**, *53*, 527−532.
(4) Schulte, G.; Fredholm, B. B. Human adenosine A(1), A(2A), A(2B), and A(3) receptors expressed in Chinese hamster ovary cells all mediate the phosphorylation of extracellular-regulated kinase 1/2. *Mol. Pharmacol.* **2000**, *58*, 477−482.
(5) Feoktistov, I.; Biaggioni, I. Adenosine A_{2B} receptors. *Pharmacol. Rev.* **1997**, *49*, 381−402.
(6) Beukers, M. W.; den Dulk, H.; van Tilburg, E. W.; Brouwer, J.; Ijzerman, A. P. Why are A(2B) receptors low-affinity adenosine receptors? Mutation of Asn273 to Tyr increases affinity of human A(2B) receptor for 2-(1-hexynyl)adenosine. *Mol. Pharmacol.* **2000**, *58*, 1349−1356.
(7) Feoktistov, I.; Biaggioni, I. Pharmacological characterization of adenosine A_{2B} receptors: studies in human mast cells co-expressing A_{2A} and A_{2B} adenosine receptor subtypes. *Biochem. Pharmacol.* **1998**, *55*, 627−633.
(8) Linden, J. New insights into the regulation of inflammation by adenosine. *J. Clin. Invest.* **2006**, *116*, 1835−1837.
(9) Zhong, H.; Wu, Y.; Belardinelli, L.; Zeng, D. A_{2B} adenosine receptors induce IL-19 from bronchial epithelial cells, resulting in TNF-alpha increase. *Am. J. Respir. Cell Mol. Biol.* **2006**, *35*, 587−592.
(10) Feoktistov, I.; Ryzhov, S.; Goldstein, A. E.; Biaggioni, I. Mast cell-mediated stimulation of angiogenesis: cooperative interaction between A_{2B} and A_3 adenosine receptors. *Circ. Res.* **2003**, *92*, 485−492.
(11) Feoktistov, I.; Ryzhov, S.; Zhong, H.; Goldstein, A. E.; Matafonov, A.; Zeng, D.; Biaggioni, I. Hypoxia modulates adenosine receptors in human endothelial and smooth muscle cells toward an A_{2B} angiogenic phenotype. *Hypertension* **2004**, *44*, 649−654.
(12) Allaman, I.; Lengacher, S.; Magistretti, P. J.; Pellerin, L. A_{2B} receptor activation promotes glycogen synthesis in astrocytes through modulation of gene expression. *Am. J. Physiol. Cell Physiol.* **2003**, *284*, 696−704.
(13) Panjehpour, M.; Castro, M.; Klotz, K.-N. Human breast cancer cell line MDA-MB-231 expresses endogenous A_{2B} adenosine receptors mediating a Ca^{2+} signal. *Br. J. Pharmacol.* **2005**, *145*, 211−218.
(14) Zablocki, J.; Elzein, E.; Kalla, R. A_{2B} adenosine receptor antagonists and their potential indications. *Exp. Opin. Ther. Pat.* **2006**, *16*, 1347−1357.
(15) Kalla, R. V.; Zablocki, J. Progress in the discovery of selective, high affinity A(2B) adenosine receptor antagonists as clinical candidates. *Purinergic Signal.* **2009**, *5*, 21−29.
(16) Kalla, R. V.; Elzein, E.; Perry, T.; Li, X.; Palle, V.; Varkhedkar, V.; Gimbel, A.; Maa, T.; Zeng, D.; Zablocki, J. Novel 1,3-disubstituted-8-(1-benzyl-1*H*-pyrazol-4-yl) xanthines: high affinity and selective A_{2B} adenosine receptor antagonists. *J. Med. Chem.* **2006**, *49*, 3682−3692.
(17) Kolachala, V.; Asamoah, V.; Wang, L.; Obertone, T. S.; Ziegler, T. R.; Merlin, D.; Sitaraman, S. V. TNF-alpha upregulates adenosine 2b (A2b) receptor expression and signaling in intestinal epithelial cells: a basis for A2bR overexpression in colitis. *Cell. Mol. Life Sci.* **2005**, *62*, 2647−2657.
(18) Strohmeier, G. R.; Reppert, S. M.; Lencer, W. I.; Madara, J. L. The A2b adenosine receptor mediates cAMP responses to adenosine receptor agonists in human intestinal epithelia. *J. Biol. Chem.* **1995**, *270*, 2387−2394.
(19) Kolachala, V.; Ruble, B.; Vijay-Kumar, M.; Wang, L.; Mwangi, S.; Figler, H.; Figler, R.; Srinivasan, S.; Gewirtz, A.; Linden, J.; Merlin, D.; Sitaraman, S. Blockade of adenosine A_{2B} receptors ameliorates murine colitis. *Br. J. Pharmacol.* **2008**, *155*, 127−137.
(20) Ryzhov, S.; Novitskiy, S. V.; Zaynagetdinov, R.; Goldstein, A. E.; Carbone, D. P.; Biaggioni, I.; Dikov, M. M.; Feoktistov, I. Host A(2B) adenosine receptors promote carcinoma growth. *Neoplasia* **2008**, *10*, 987−995.
(21) Ortore, G.; Martinelli, A. A_{2B} receptor ligands: past, present and future trends. *Curr. Top. Med. Chem.* **2010**, *10*, 923−940.
(22) Kalla, R. V.; Zablocki, J.; Tabrizi, M. A.; Baraldi, P. G. Recent developments in A_{2B} adenosine receptor ligands. *Handb. Exp. Pharmacol.* **2009**, 99−122.
(23) Stefanachi, A.; Brea, J. M.; Cadavid, M. I.; Centeno, N. B.; Esteve, C.; Loza, M. I.; Martinez, A.; Nieto, R.; Ravina, E.; Sanz, F.; Segarra, V.; Sotelo, E.; Vidal, B.; Carotti, A. 1-, 3- and 8-Substituted-9-deazaxanthines as potent and selective antagonists at the human A_{2B} adenosine receptor. *Bioorg. Med. Chem.* **2008**, *16*, 2852−2869.
(24) Castelhano, A. L.; Mckibben, B.; Steinig, A. G. Preparation of pyrrolopyrimidine A2b selective antagonist compounds, method of synthesis and therapeutic use. PCT Int. Appl. WO 2003053361, 2003.
(25) Pastorin, G.; Da Ros, T.; Spalluto, G.; Deflorian, F.; Moro, S.; Cacciari, B.; Baraldi, P. G.; Gessi, S.; Varani, K.; Borea, P. A. Pyrazolo[4,3-*e*]-1,2,4-triazolo[1,5-*c*]pyrimidine derivatives as adenosine receptor antagonists. Influence of the N5 substituent on the affinity at the human A_3 and A_{2B} adenosine receptor subtypes: a molecular modeling investigation. *J. Med. Chem.* **2003**, *46*, 4287−4296.
(26) Vidal, J.; Bernat, E.; Trias, C. Preparation of pyrimidin-2-amines as A_{2B} adenosine receptor antagonists. PCT Int. Appl. WO 2005040155, 2005.
(27) Vidal, B.; Nueda, A.; Esteve, C.; Domenech, T.; Benito, S.; Reinoso, R. F.; Pont, M.; Calbet, M.; Lopez, R.; Cadavid, M. I.; Loza, M. I.; Cardenas, A.; Godessart, N.; Beleta, J.; Warrellow, G.; Ryder, H. Discovery and characterization of 4′-(2-furyl)-*N*-pyridin-3-yl-4,5′-bipyrimidin-2′-amine (LAS38096), a potent, selective, and efficacious

A_{2B} adenosine receptor antagonist. *J. Med. Chem.* **2007**, *50*, 2732−2736.
(28) Da Settimo, F.; Primofiore, G.; Taliani, S.; Marini, A. M.; La Motta, C.; Novellino, E.; Greco, G.; Lavecchia, A.; Trincavelli, L.; Martini, C. 3-Aryl[1,2,4]triazino[4,3-*a*]benzimidazol-4(10*H*)-ones: a new class of selective A_1 adenosine receptor antagonists. *J. Med. Chem.* **2001**, *44*, 316−327.
(29) Da Settimo, F.; Primofiore, G.; Taliani, S.; La Motta, C.; Novellino, E.; Greco, G.; Lavecchia, A.; Cosimelli, B.; Iadanza, M.; Klotz, K.-N.; Tuscano, D.; Trincavelli, M. L.; Martini, C. A_1 adenosine receptor antagonists, 3-aryl[1,2,4]triazino[4,3-*a*]benzimidazol-4-(10*H*)-ones (ATBIs) and *N*-alkyl and *N*-acyl-(7-substituted-2-phenylimidazo[1,2-*a*][1,3,5]triazin-4-yl)amines (ITAs): different recognition of bovine and human binding sites. *Drug Dev. Res.* **2004**, *63*, 1−7.
(30) Novellino, E.; Abignente, E.; Cosimelli, B.; Greco, G.; Iadanza, M.; Laneri, S.; Lavecchia, A.; Rimoli, M. G.; Da Settimo, F.; Primofiore, G.; Tuscano, D.; Trincavelli, L.; Martini, C. Design, synthesis and biological evaluation of novel *N*-alkyl- and *N*-acyl-(7-substituted-2-phenylimidazo[1,2-*a*][1,3,5]triazin-4-yl)amines (ITAs) as novel A(1) adenosine receptor antagonists. *J. Med. Chem.* **2002**, *45*, 5030−5036.
(31) Novellino, E.; Cosimelli, B.; Ehlardo, M.; Greco, G.; Iadanza, M.; Lavecchia, A.; Rimoli, M. G.; Sala, A.; Da Settimo, A.; Primofiore, G.; Da Settimo, F.; Taliani, S.; La Motta, C.; Klotz, K. N.; Tuscano, D.; Trincavelli, M. L.; Martini, C. 2-(Benzimidazol-2-yl)quinoxalines: a novel class of selective antagonists at human A(1) and A(3) adenosine receptors designed by 3D database searching. *J. Med. Chem.* **2005**, *48*, 8253−8260.
(32) Da Settimo, F.; Primofiore, G.; Taliani, S.; Marini, A. M.; La Motta, C.; Simorini, F.; Salerno, S.; Sergianni, V.; Tuccinardi, T.; Martinelli, A.; Cosimelli, B.; Greco, G.; Novellino, E.; Ciampi, O.; Trincavelli, M. L.; Martini, C. 5-Amino-2-phenyl[1,2,3]triazolo[1,2-*a*][1,2,4]benzotriazin-1-one: a versatile scaffold to obtain potent and selective A_3 adenosine receptor antagonists. *J. Med. Chem.* **2007**, *50*, 5676−5684.
(33) Cosimelli, B.; Greco, G.; Ehlardo, M.; Novellino, E.; Da Settimo, F.; Taliani, S.; La Motta, C.; Bellandi, M.; Tuccinardi, T.; Martinelli, A.; Ciampi, O.; Trincavelli, M. L.; Martini, C. Derivatives of 4-amino-6-hydroxy-2-mercaptopyrimidine as novel, potent, and selective A_3 adenosine receptor antagonists. *J. Med. Chem.* **2008**, *51*, 1764−1770.
(34) Taliani, S.; La Motta, C.; Mugnaini, L.; Simorini, F.; Salerno, S.; Marini, A. M.; Da Settimo, F.; Cosconati, S.; Cosimelli, B.; Greco, G.; Limongelli, V.; Marinelli, L.; Novellino, E.; Ciampi, O.; Daniele, S.; Trincavelli, M. L.; Martini, C. Novel N2-substituted pyrazolo[3,4-*d*]pyrimidine adenosine A_3 receptor antagonists: inhibition of A_3-mediated human glioblastoma cell proliferation. *J. Med. Chem.* **2010**, *53*, 3954−3963.
(35) Frick, J. S.; MacManus, C. F.; Scully, M.; Glover, L. E.; Eltzschig, H. K.; Colgan, S. P. Contribution of adenosine A_{2B} receptors to inflammatory parameters of experimental colitis. *J. Immunol.* **2009**, *182*, 4957−4964.
(36) Primofiore, G.; Da Settimo, F.; Taliani, S.; Marini, A. M.; La Motta, C.; Novellino, E.; Greco, G.; Gesi, M.; Trincavelli, L.; Martini, C. 3-Aryl-[1,2,4]triazino[4,3-*a*]benzimidazol-4(10*H*)-ones: tricyclic heteroaromatic derivatives as a new class of benzodiazepine receptor ligands. *J. Med. Chem.* **2000**, *43*, 96−102.
(37) Schelz, D. Synthesis of 1-aryl- and 1-alkyl-2,3-dimethylquinoxalinium perchlorates. 2. Synthesis and proton NMR spectra of 2,3-dimethyl-1-phenyl-6-X-quinoxalinium perchlorates. *Helv. Chim. Acta* **1978**, *61*, 2452−2462.
(38) Parihar, H. S.; Suryanarayanan, A.; Ma, C.; Joshi, P.; Venkataraman, P.; Schulte, M. K.; Kirschbaum, K. S. 5-HT(3)R binding of lerisetron: an interdisciplinary approach to drug−receptor interactions. *Bioorg. Med. Chem. Lett.* **2001**, *11*, 2133−2136.
(39) Jaakola, V. P.; Griffith, M. T.; Hanson, M. A.; Cherezov, V.; Chien, E. Y.; Lane, J. R.; Ijzerman, A. P.; Stevens, R. C. The 2.6 angstrom crystal structure of a human A_{2A} adenosine receptor bound to an antagonist. *Science* **2008**, *322*, 1211−1217.
(40) Lenzi, O.; Colotta, V.; Catarzi, D.; Varano, F.; Poli, D.; Filacchioni, G.; Varani, K.; Vincenzi, F.; Borea, P. A.; Paoletta, S.; Morizzo, E.; Moro, S. 2-Phenylpyrazolo[4,3-*d*]pyrimidin-7-one as a new scaffold to obtain potent and selective human A_3 adenosine receptor antagonists: new insights into the receptor−antagonist recognition. *J. Med. Chem.* **2009**, *52*, 7640−7652.
(41) Tosh, D. K.; Chinn, M.; Ivanov, A. A.; Klutz, A. M.; Gao, Z. G.; Jacobson, K. A. Functionalized congeners of A_3 adenosine receptor-selective nucleosides containing a bicyclo[3.1.0]hexane ring system. *J. Med. Chem.* **2009**, *52*, 7580−7592.
(42) Kim, J.; Wess, J.; van Rhee, A. M.; Schoneberg, T.; Jacobson, K. A. Site-directed mutagenesis identifies residues involved in ligand recognition in the human A_{2a} adenosine receptor. *J. Biol. Chem.* **1995**, *270*, 13987−13997.
(43) Lin, S. W.; Sakmar, T. P. Specific tryptophan UV-absorbance changes are probes of the transition of rhodopsin to its active state. *Biochemistry* **1996**, *35*, 11149−11159.
(44) Audet, M.; Bouvier, M. Insights into signaling from the beta2-adrenergic receptor structure. *Nature Chem. Biol.* **2008**, *4*, 397−403.
(45) Xu, F.; Wu, H.; Katritch, V.; Han, G. W.; Jacobson, K. A.; Gao, Z. G.; Cherezov, V.; Stevens, R. C. Structure of an agonist-bound human A_{2A} adenosine receptor. *Science* **2011**, *332*, 322−327.
(46) Sherbiny, F. F; Schiedel, A. C.; Maass, A.; Müller, C. E. Homology modelling of the human adenosine A_{2B} receptor based on X-ray structures of bovine rhodopsin, the β_2-adrenergic receptor and the human adenosine A_{2A} receptor. *J. Comput.-Aided. Mol. Des.* **2009**, *23*, 807−828.
(47) Cheng, F.; Xu, Z.; Liu, G.; Tang, Y. Insights into binding modes of adenosine A_{2B} antagonists with ligand-based and receptor-based methods. *Eur. J. Med. Chem.* **2010**, *45*, 3459−3471.
(48) Iemura, R.; Kawashima, T.; Fukuda, T.; Ito, K.; Tsukamoto, G. Synthesis of 2-(4-substituted-1-piperazinyl)benzimidazoles as H1-antihistaminic agents. *J. Med. Chem.* **1986**, *29*, 1178−1183.
(49) Dembeck, P.; Ricci, A.; Seconi, G.; Vivarelli, P. Studies on benzimidazoles. Part VII: Kinetics and mechanism of the reaction of thiophenoxydehalogenation of *N*,*N*′-disubstituted 2-chlorobenzimidazolium perchlorates. *J. Chem. Soc. B* **1971**, 557−560.
(50) Barbero, N.; Carril, M.; SanMartin, R.; Dominguez, E. Copper-catalyzed intramolecular *N*-arylation of ureas in water: a novel entry to benzoimidazolones. *Tetrahedron* **2008**, *64*, 7283−7288.
(51) Bianchi, M.; Butti, A.; Rossi, S.; Barzaghi, F.; Marcaria, V. Compounds with antiulcer and antisecretory activity. I. 3-Arylbenzimidazolin-2-ones and -thiones. *Eur. J. Med. Chem.* **1981**, *16*, 321−326.
(52) Klotz, K.-N.; Hessling, J.; Hegler, J.; Owman, C.; Kull, B.; Fredholm, B. B.; Lohse, M. J. Comparative pharmacology of human adenosine receptor subtypes—characterization of stably transfected receptors in CHO cells. *Naunyn Schmiedeberg's Arch. Pharmacol.* **1998**, *357*, 1−9.
(53) Cheng, Y.; Prusoff, W. H. Relationship between the inhibition constant (K_1) and the concentration of inhibitor which causes 50% inhibition (I_{50}) of an enzymatic reaction. *Biochem. Pharmacol.* **1973**, *22*, 3099−3108.
(54) Nordstedt, C.; Fredholm, B. B. A modification of a protein-binding method for rapid quantification of cAMP in cell-culture supernatants and body fluid. *Anal. Biochem.* **1990**, *189*, 231−234.
(55) Lovell, S. C.; Davis, I. W.; Arendall, W. B.; de Bakker, P. I.; Word, J. M.; Prisant, M. G.; Richardson, J. S.; Richardson, D. C. Structure validation by Calpha geometry: phi,psi and Cbeta deviation. *Proteins* **2003**, *50*, 437−450.
(56) *Prime*; Schrödinger, LLC: New York, 2005.
(57) *Maestro*; Schrödinger, LLC: New York, 2006.
(58) Jacobson, M. P.; Pincus, D. L.; Rapp, C. S.; Day, T. J.; Honig, B.; Shaw, D. E.; Friesner, R. A. A hierarchical approach to all-atom protein loop prediction. *Proteins* **2004**, *55*, 351−367.